

Composition and compatibilization induced morphology alteration in PVDF/LLDPE blends: correlation between rheology and morphology

A. Jameie Oskooie^{1,2} · M. K. Razavi Aghjeh^{1,2} · O. Rafeie^{1,2} · A. Tavakoli³

Received: 18 October 2016 / Accepted: 4 January 2017 / Published online: 9 January 2017
© Springer Science+Business Media Dordrecht 2017

Abstract Correlation between the rheology and morphology of PVDF/LLDPE blends as well as the effect of LLDPE-g-MA compatibilizer on the microstructure and viscoelastic properties of these blends were studied in detail. Morphology development from matrix-dispersed to co-continuous and again to dispersed-matrix was well predicted using various linear viscoelastic analyses and confirmed via direct SEM experiments and continuity index analysis. Compatibilization induced alteration in the microstructure of the blends, particularly PVDF/PE 50/50 blend from co-continuous morphology to dispersed-matrix one, was also concluded from viscoelastic analysis and confirmed. It was shown that the feeding order had a distinct effect on morphology of the blends near the phase inversion composition. “Phase within a phase within a phase” morphology was observed near the phase inversion region, provided that the components are fed simultaneously. Different melting and crystallization temperature range of PVDF and PE phases was understood to be the main reason of this observation. It was also shown that compatibilization had higher impact on LLDPE-rich blends than PVDF-rich blends, while narrowed the co-continuity composition range.

Keywords PVDF/PE blends · Rheology · Morphology · Compatibilization · Co-continues morphology

✉ M. K. Razavi Aghjeh
karimrazavi@sut.ac.ir

¹ Institute of Polymeric Materials, Sahand University of Technology, Sahand New Town, Tabriz 51335-1996, Iran

² Faculty of Polymer Engineering, Sahand University of Technology, Sahand New Town, Tabriz 51335-1996, Iran

³ Chemical Engineering Department, Sahand University of Technology, Sahand New Town, Tabriz 51335-1996, Iran

Introduction

Blending of two or more polymers to obtain a new polymer is a known route to develop new materials with desirable properties [1–5]. It has clearly been understood that most of properties of immiscible polymer blends are mainly controlled by the morphology as well as the interfacial interaction between phases. On the other hand, the morphology is dependent on composition, viscoelastic properties of the components, extent of deformation flow field and compatibility [6, 7]. The dominant mechanisms in morphology development of an immiscible polymer blend are elongation of molten droplets into fibrous styles, breaking down of the fibrous domains into smaller droplets and coalescence of these small droplets. Equilibrium between these mechanisms determines the final morphology of an immiscible polymer blend [6].

Among different morphology states of immiscible polymer blends, matrix-dispersed and co-continues microstructures are two most known types of morphology. Co-continuous morphology is usually formed around the unstable phase inversion composition region in which both the components exhibit high degree of continuity, one inside the other. The blends of co-continuous morphology are of particularly important in cases that one phase is barrier [8] or conductive [9]. In latter case, the continuity of conductive phase would result in conductivity of the blend. For instance, in various research works [10–12], efforts have been made to determine the composition range of co-continuity to be able to benefit from “double percolation” concept. Double-percolation concept refers to the microstructure in which conductive filler selectively localizes and forms a three dimensional network in one phase or at the interface of a polymer blend consisting of co-continuous morphology [13–15].

Polyvinylidene fluoride (PVDF) is a semi-crystalline thermoplastic which combines excellent chemical and thermal

resistance, high mechanical strength and dielectric permittivity and unique pyro and piezo-electric properties [16–18], which make it suitable in various applications such as micro-electromechanical devices, high-charge storage capacitors, coatings, polymer processing additives, pipes, valves, etc. [19]. However, high cost and low production volume of this polymer are its drawbacks. Blending of PVDF with a suitable polymer can be an effective strategy to overcome these drawbacks. In this way, polyethylene can be a good choice, since it has high chemical resistance, good processability and relatively good dielectric permittivity, while it could cover the drawbacks of the PVDF [17–19]. M. Kaseem et al. [20] studied the rheological properties of PVDF/LDPE blends and showed that the PVDF/LDPE blends are incompatible. They reported that the co-continuous morphology was formed at 50/50 composition. X. Lin et al. [19] showed that the interfacial interaction between PVDF and LDPE phases and consequently the electrical properties of their blends were improved in the presence of LDPE-g-MA as an interfacial agent.

In this research work, correlation between the rheology and morphology of PVDF/LLDPE blends and the effect of LLDPE-g-MA on the microstructure and viscoelastic properties of the blends were systematically studied, in a wide range of compositions. The composition range of co-continuous morphology was also determined via indirect viscoelastic analysis and examined directly using microscopic observations. Following to this work, the results of an interesting research work focusing on rheology, morphology and conductive behavior of PVDF/LLDPE/Graphene blend nanocomposites, at compositions near the co-continuity, will be presented.

Experimental

Materials

The PVDF (Kynar, $M_w = 70,000$ and $M_w/M_n = 2$) from Arkema, Paris, France and LLDPE (MFI = 0.9 g/10 min; 190 °C, 2.160 kg) from Tabriz Petrochemical Company, Iran, marked as PE hereinafter, were used as the base materials. Maleic anhydride grafted LLDPE (LLDPE-g-MA; E-119 MFI = 1.9 g/10 min; 190 °C, 2.160 kg), denoted as PEMA hereinafter, purchased from Pluss Polymers, India, was used as compatibilizer. N, N Dimethylformamide (DMF) from Daejung Co., Korea and xylene from Dr. Mojallali Co., Iran were used as the solvents of PVDF and LLDPE phases, respectively.

Blend preparation

To avoid the effect of moisture, all the components were dried in a vacuum oven for 24 h at 80 °C, prior to melt blending. All the samples were prepared in an internal mixer (Brabender

W50EHT) with a rotor speed of 60 rpm at starting temperature of 190 °C. All the polymeric components were first dry mixed and then fed into the chamber and blended for 10 min (feeding order: 1), unless otherwise specified. In some cases, to study the effect of blending sequence on morphology development, some samples were prepared using two other different feeding orders. For this purpose, the PE phase was first fed into the chamber and after its plastification, the PVDF phase was incorporated and compounding was continued for 10 min (feeding order: 2) and in another feeding order the PE phase was fed after melt mixing of PVDF phase at the same conditions (feeding order: 3). The pure PVDF and PE were also processed under the same conditions, for comparison. For compatibilized blends 5 wt% of PE phase was replaced by PEMA. Different prepared compositions with the corresponding codes are listed in Table 1. A small amount of each prepared blend samples was rapidly quenched in liquid nitrogen for morphological studies. The obtained samples were compression-molded into suitable pieces for rheological analysis. Molding was carried out at 190 °C followed by slow water cooling under 100 bar pressure.

Characterization

Rheological studies

Dynamic melt rheological measurements were carried out using a dynamic rheometer (MCR301: Anton Paar) equipped with parallel plate geometry (diameter = 25 mm, gap = 1 mm). The frequency sweep tests were performed in the range of 0.04 ~ 625 $\text{rad}\cdot\text{sec}^{-1}$ at fixed temperature of 200 °C with an amplitude of 1% in order to maintain the response of the materials in the linear viscoelastic regime. The measurements were conducted under nitrogen gas flow to avoid premature thermal degradation of the samples.

Continuity index analysis

Continuity index of the PVDF and PE phases in different blends was determined using selective extraction method [5, 21–23]. Samples of specified weight of each blend were stirred in DMF solvent for 48 h at a constant temperature of 60 °C to selectively extract the PVDF phase. The samples were also extracted in boiling xylene for 12 h to extract the PE phase. The continuity index of the considered component (PVDF or PE) was quantified using the following equation:

$$CI_{\text{Polymer}} = \frac{m_{\text{ini}} - m_{\text{ext}}}{m_{\text{ini}}} \times 100$$

where, m_{ini} is the weight of the considered component initially present in the blend and m_{ext} the weight of the same component in the blend after extraction. The reported value was the

Table 1 Different prepared samples, the corresponding codes and employed feeding orders

Code	PVDF	LLDPE	LLDPE-g-MA	Feeding order
PVDF	100	0	0	1
PVDF/PE 80/20	80	20	0	1
PVDF/PE 70/30	70	30	0	1
PVDF/PE 60/40	60	40	0	1
PVDF/PE 50/50	50	50	0	1
PVDF/PE 40/60	40	60	0	1
PVDF/PE 20/80	20	80	0	1
PE	0	100	0	1
PVDF/PE/PEMA 80/15/5	80	15	5	1
PVDF/PE/PEMA 70/25/5	70	25	5	1
PVDF/PE/PEMA 60/35/5	60	35	5	1
PVDF/PE/PEMA 50/45/5	50	45	5	1
PVDF/PE/PEMA 40/55/5	40	55	5	1
PVDF/PE/PEMA 20/75/5	20	75	5	1
PVDF/(PE) 50/50	50	50	0	2
(PVDF)/PE 50/50	50	50	0	3

average of at least three samples with the same composition. When the sample was not disintegrated after the PVDF or PE phase extraction, the PE or PVDF phases were considered as 100% continuous phase, respectively and the continuity index of the other phase was quantified from the equation.

Morphology observation

Morphology of the blends was examined using scanning electron microscopy method (SEM; VEGA, TESCAN). Only the cryo-fractured surface of the PE-rich blends was selectively extracted with DMF for 24 h at 60 °C for removal of the PVDF phase. Then the fractured surfaces were coated with a thin layer of gold to avoid electrostatic charging during examination and then micrographs were taken with different magnifications.

Result and discussion

Rheological studies

The storage modulus of different PVDF/PE blends along with the same results for the pure PVDF and PE are shown in Fig. 1. The results of complex viscosity were excluded for brevity. The results show that both pure polymers exhibit a power law type behavior as shear-thinning materials and the PE shows higher elasticity than the pure PVDF. Although all the PVDF/PE blends of different compositions indicate shear-thinning behavior, alteration in rheological behavior of various blends is obvious, particularly at low frequency ranges.

This alteration is mainly due to additional relaxation processes [24–26]. Decreasing the dependency of elasticity at low frequencies from ($G \sim \omega^2$) for pure components to ($G \sim \omega^{-2}$) in immiscible polymer blends, is in the results of shape relaxation of dispersed particles and/or complicated interfacial relaxation phenomenon [24, 26].

The slope of the storage modulus (SSM) at low frequency ranges was calculated for different PVDF/PE blends and plotted versus PVDF content (Fig. 2). As it can clearly be seen, the SSM smoothly decreases with PVDF content and increases again after passing through a minimum around PVDF/PE 60/40 composition. This change in rheological behavior can be attributed to the change in the morphology of the blends, since it has clearly been understood that the rheological behavior of

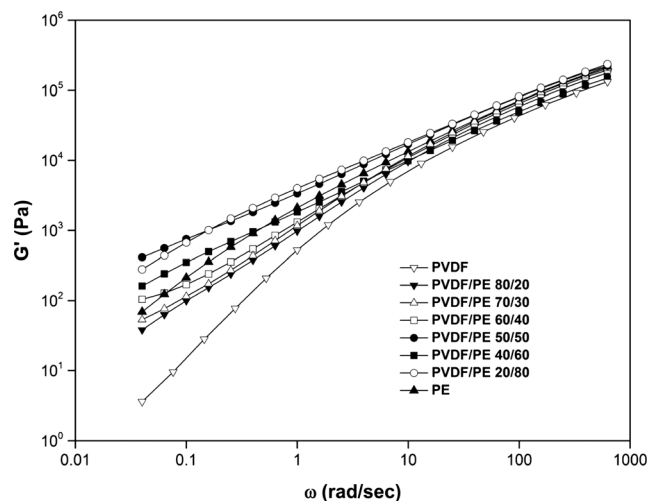


Fig. 1 Storage modulus versus angular frequency for different PVDF/PE blends

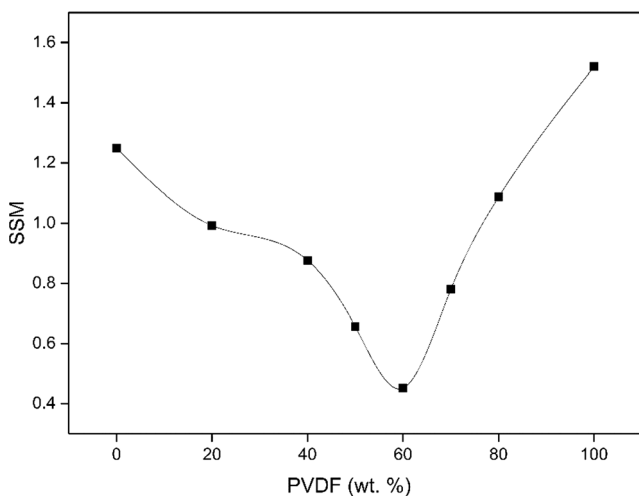


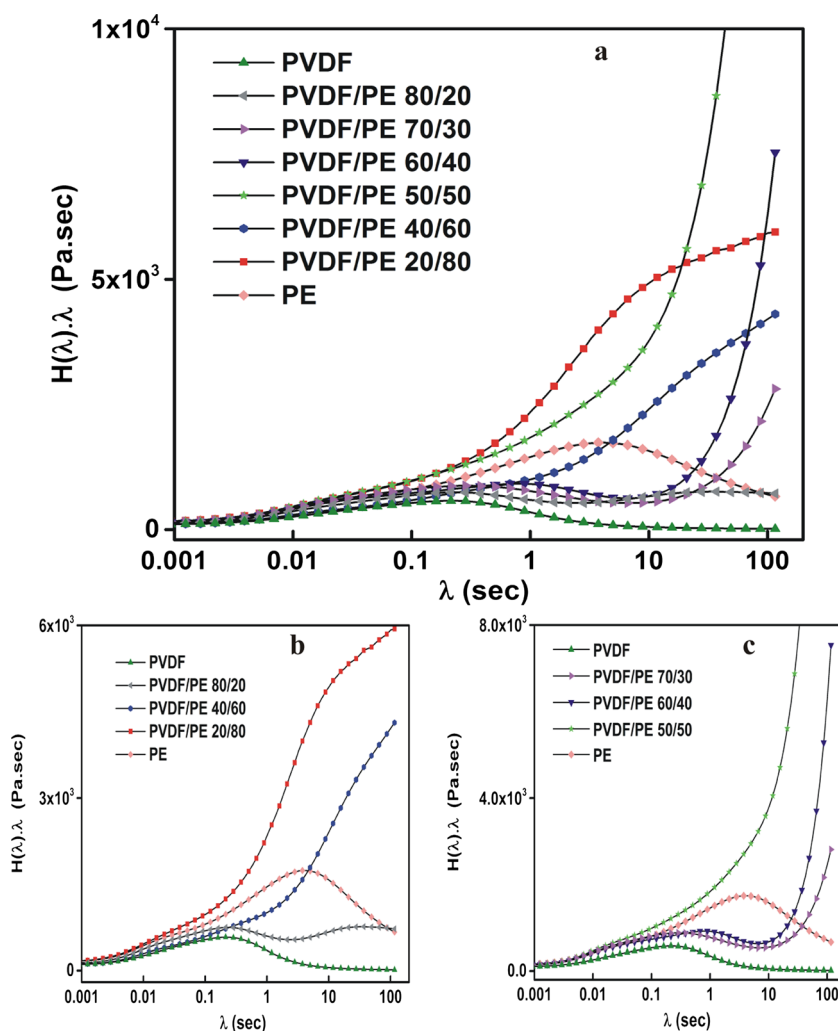
Fig. 2 Slope of the storage modulus (SSM) at low frequency ranges for PVDF/PE blends versus PVDF content

immiscible polymer blends is widely affected by the blend microstructure as well as interfacial interaction between

phases [5, 27]. D. Wu [28] showed that the linear dynamic rheological properties can give more accurate information on the phase inversion of polymer blends. From the results of Fig. 2, it can be preliminarily guessed that the matrix-dispersed morphology at low PVDF contents, alters to co-continuous morphology at intermediate compositions (around 60 wt% of PVDF) and changes again to matrix-dispersed after phase inversion.

Figure 3 shows the relaxation time spectra of the pure PVDF and PE along with the same results for different blends. The relaxation peak of the PVDF appears at shorter relaxation times than that of PE, which can be possibly related to the lower molecular weight of PVDF and/or different polarity and flexibility of the PVDF and PE chains. Relaxation time spectra of PVDF/PE 80/20, 40/60 and 20/80 blends exhibit the relaxation characteristics of an immiscible blend consisting of matrix-dispersed morphology (Fig. 3b). In these spectra the first peak is related to the relaxation of the polymeric macromolecules (chains) and the second wide peak, appeared at higher relaxation times, is associated with the shape relaxation

Fig. 3 Relaxation spectra of PVDF/PE blends in various compositions



of dispersed particles. It should be noted that due to overlapping of the relaxation peaks, the first peak for 40/60 and 20/80 are not clear in this figure. However in logarithmic scales for the $H(\lambda) \cdot \lambda$, which are not presented here, two relaxation peaks are visible. For the rest of compositions (PVDF/PE 70/30, 60/40 and 50/50) a clear relaxation peak, associated with the shape relaxation of dispersed particles, has not been appeared at the time scales of experiments (max 100 s) and the values of $H(\lambda) \cdot \lambda$ goes to infinity (Fig. 3c), representative of the complicated interfacial relaxation phenomena in these compositions. This can be a sign of co-continuous morphology and/or dispersion of interconnected big particles in these compositions [29].

Effect of PEMA on viscoelastic properties of various PVDF/PE blends is illustrated in Figs. 4 and 5.

As can be seen, addition of PEMA to PVDF/PE 80/20 blend increased the storage modulus and decreased $\tan \delta$ at low frequencies, where the effect of interfacial interaction on rheological characteristics of the multiphase systems is more pronounced. The $\tan \delta$ peak also shifted to higher frequencies (low relaxation times) upon addition of PEMA. These are indicative of compatibilizing effect of PEMA. PEMA had less effect on rheological behaviors of PVDF/PE 70/30 and 60/40 blends, compared to PVDF/PE 80/20 blend, may be due to the higher interfacial area in the former blends. Improvement of the interfacial interaction in PVDF/PE 40/60 and 20/80 blends upon addition of PEMA can also be concluded from the

Fig. 4 Effect of 5 wt.% PEMA compatibilizer on storage modulus of PVDF/PE blends: **a** 80/20, **b** 70/30, **c** 60/40, **d** 50/50, **e** 40/60 and **f** 20/80

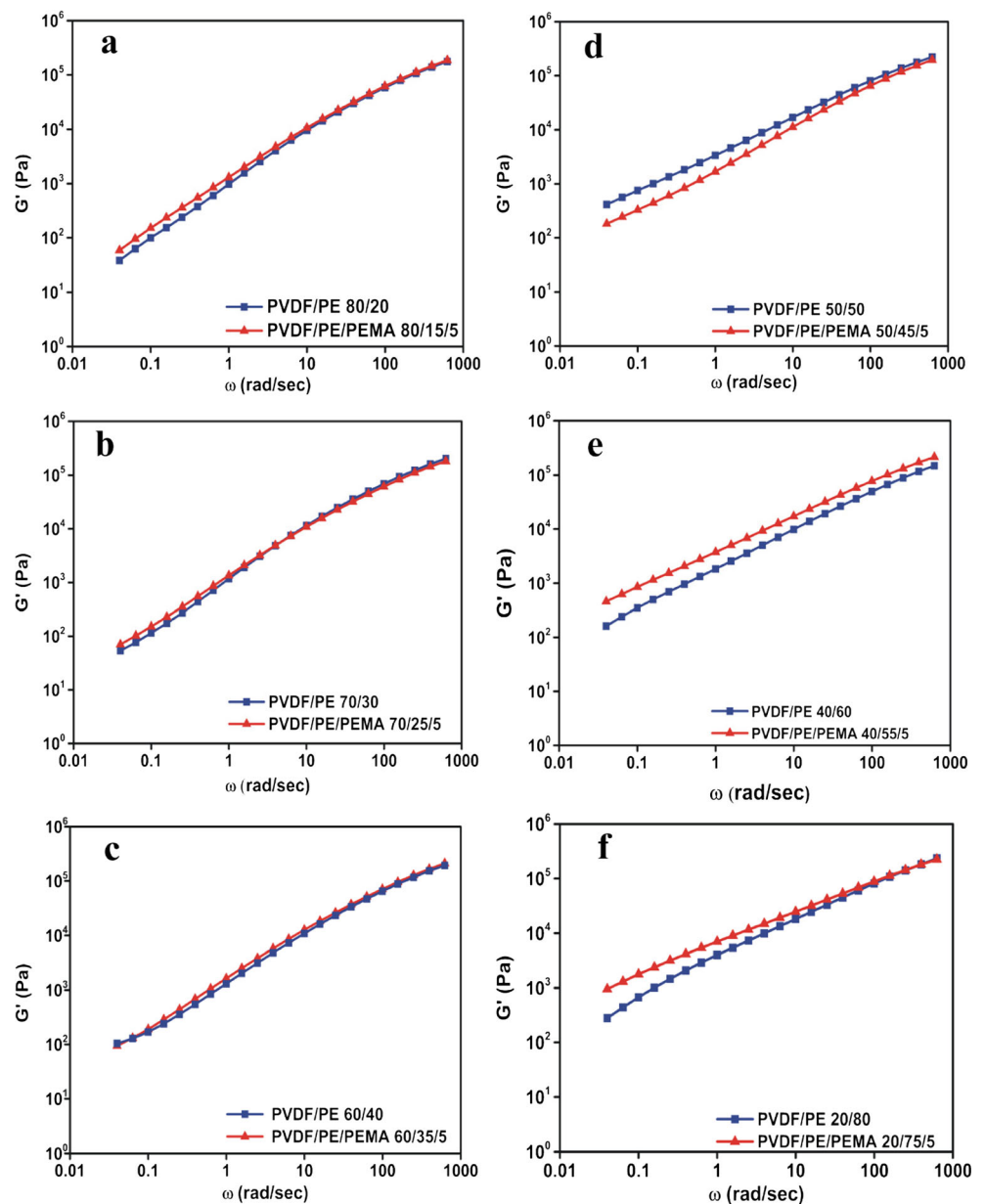
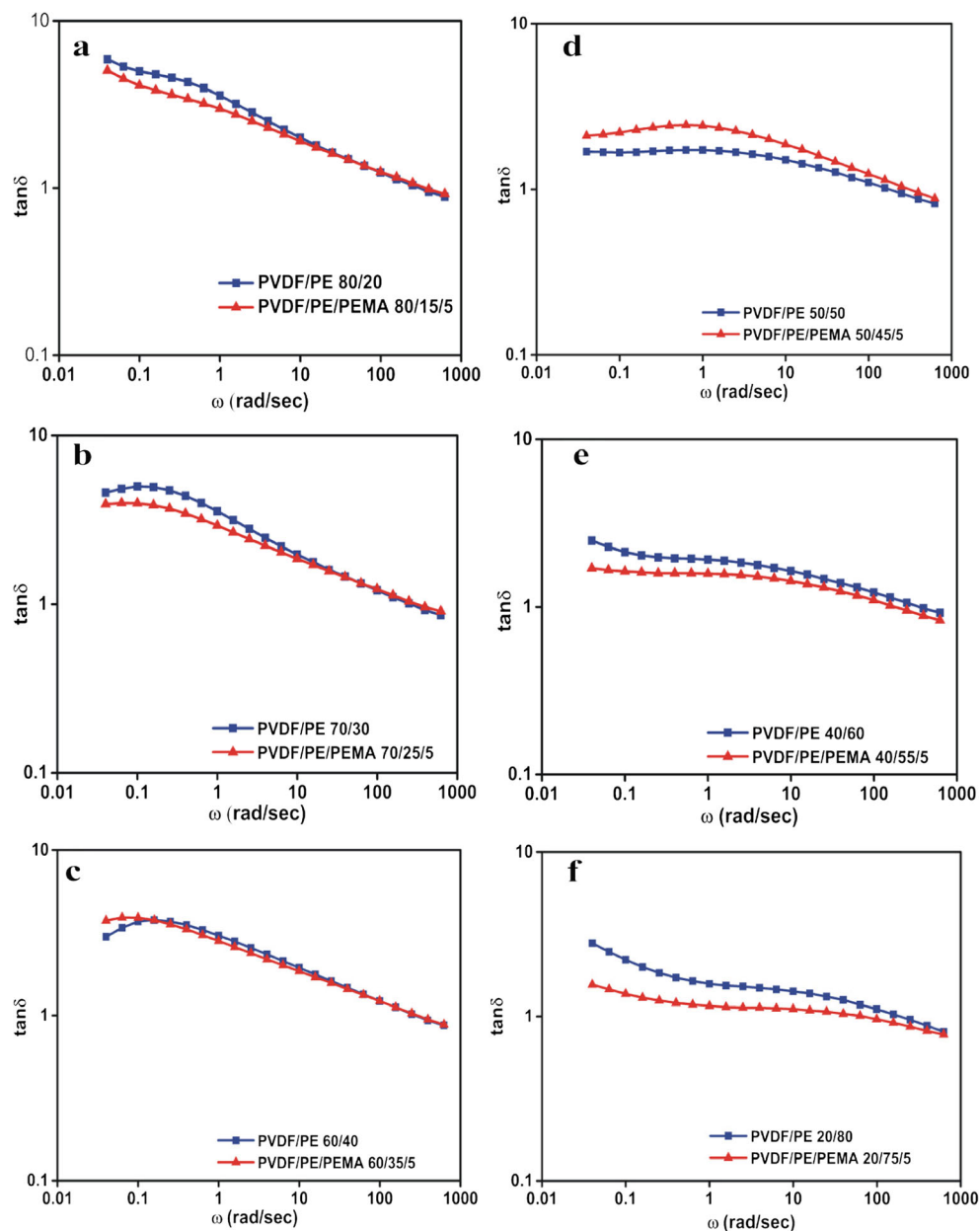


Fig. 5 Effect of 5 wt.% PEMA compatibilizer on damping factor of PVDF/PE blends: **a** 80/20, **b** 70/30, **c** 60/40, **d** 50/50, **e** 40/60 and **f** 20/80



results. Moreover, the results indicate that the effect of PEMA on PE-rich blends is higher than those of PVDF-rich blends. Contrary to the previously studied blends [5, 19, 24], PEMA decreased the storage modulus and increased the $\tan \delta$ of PVDF/PE 50/50 blend, may be due to possible alteration in morphological features of the sample after addition of PEMA, since the composition may fall in the unstable phase inversion region (Fig. 2). This will be evident in morphological studies.

Continuity index analysis

Figure 6 presents the continuity index of PVDF and PE components in the un-compatibilized and compatibilized PVDF/PE blends as functions of PVDF content. It is obvious that the

PVDF phase is continuous over the composition range of 60 ~ 100 wt% PVDF and the PE phase exhibits continuity between 0 ~ 60 wt.% PVDF in un-compatibilized blends. For PVDF/PE 50/50 blend, PE phase exhibits 100% continuity, whereas the PVDF phase shows 25% continuity. In PVDF/PE 70/30 blend, PVDF and PE phases exhibits 100 and 60% continuity, respectively. Therefore it can be claimed that un-compatibilized PVDF/PE blends exhibit co-continuity between 50 ~ 70% of PVDF phase. Upon the addition of PEMA, PVDF phase exhibited 0% continuity in PVDF/PE 50/50 blend, representative of alteration of morphology from co-continuous to matrix-dispersed in this composition as a result of compatibilization. This alteration justifies decreased storage modulus and increased $\tan \delta$ for this composition after

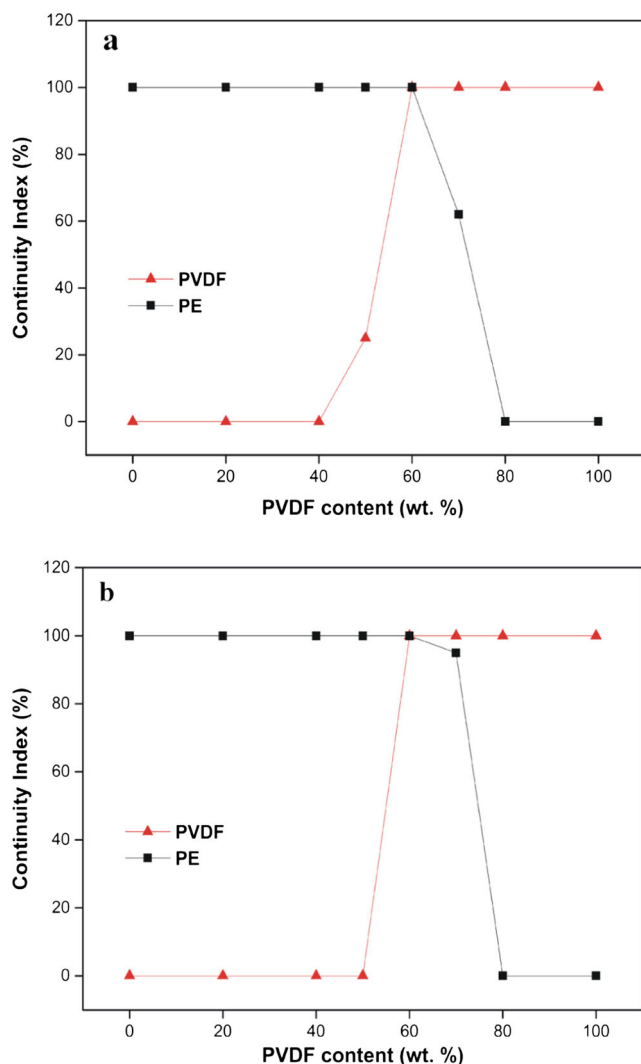


Fig. 6 Continuity index of PVDF and PE phases in **a** un-compatibilized and **b** compatibilized PVDF/PE blends as functions of PVDF content

PEMA addition (Figs. 4 and 5). Compatibilization did not change the continuity indexes of PVDF and PE phases in PVDF/PE 60/40 blend showing of preserved morphology state during compatibilization. For PVDF/PE 70/30 blend, the continuity index of PE phase increased to 95% while the PVDF phase remained 100% continuous after compatibilization. The final conclusion of these statements is that compatibilization narrowed the co-continuity composition range from 50 ~ 70% to 60 ~ 70% of PVDF phase and the phase inversion is taken placed near the PVDF/PE 60/40 composition. These results also show a good agreement with the results of rheological analysis.

SEM observations

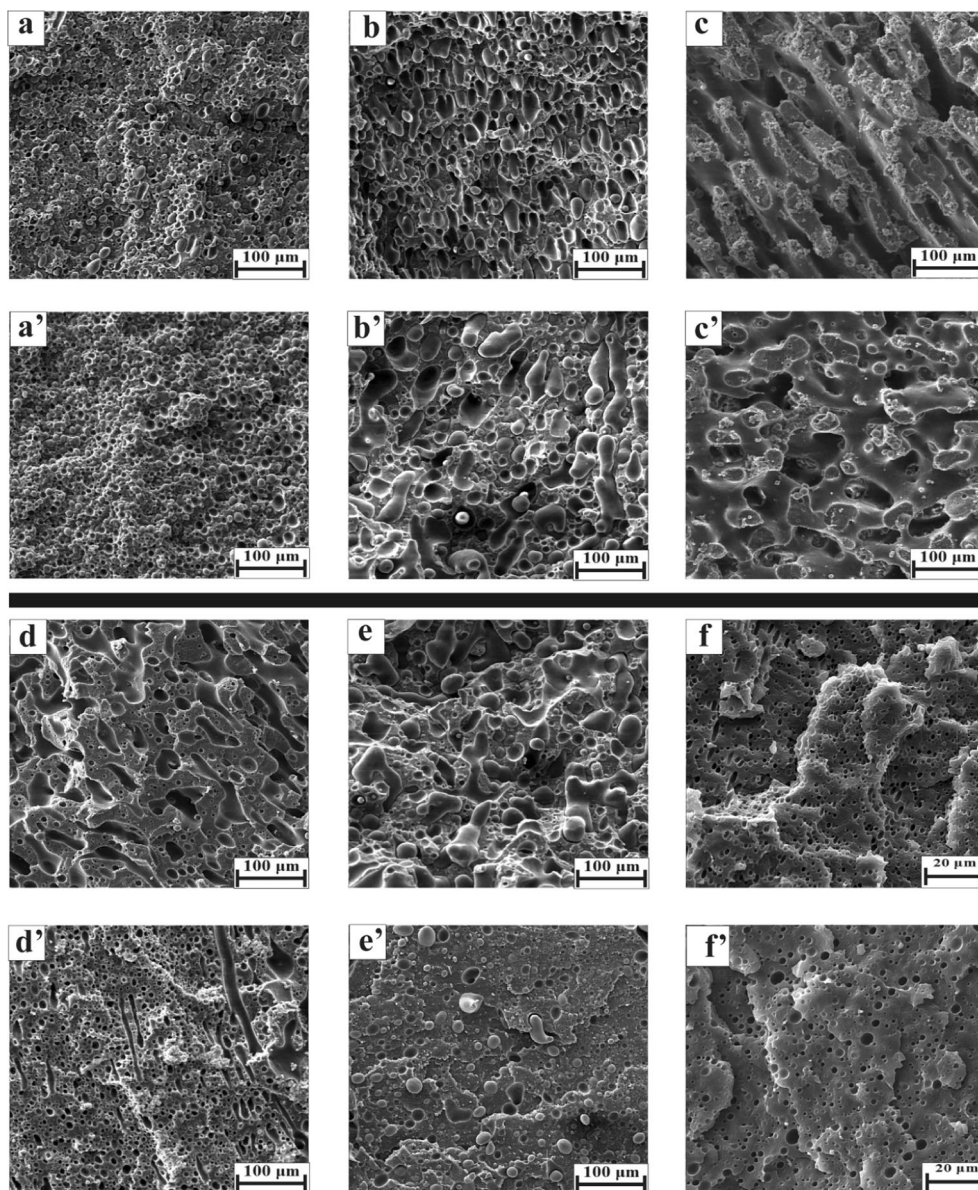
Figure 7 shows the SEM micrographs of cryo-fractured surfaces of the un-compatibilized and corresponding compatibilized PVDF/PE blends at different compositions.

For better contrast in some samples (PVDF/PE 20/80, 40/60, 50/50, 60/40 and PVDF/PE/PEMA 20/75/5, 40/55/5, 50/45/5, 60/35/5 blends), the PVDF phase was etched by DMF solvent. A matrix-dispersed morphology is obvious for the PVDF/PE 80/20 blend, in which the spherical PE particles are dispersed in the PVDF matrix. For the PVDF/PE 70/30 blend, the dispersed PE domains clearly exhibit elongated or fibrous structures. Both the PVDF and PE phases formed continuous phase structure, as the PE content increased to 40 wt.%. In the PVDF/PE 50/50 blend, the PVDF phase displays fibrous-like and/or formless dispersed domains in PE matrix. In other word, the morphology of the 50/50 blend can be considered as semi co-continuous morphology. Further increase in PE content led to dispersion of spherical dispersed droplets of the minor PVDF phase in the PE matrix for PVDF/PE 40/60 and 20/80 blends. These results suggest that PVDF and PE phases basically form the co-continuous structure in the composition region of 50 ~ 70% of the PVDF phase, confirming the results of continuity index analysis. As expected, the domain size of the less viscous PVDF phase for PVDF/PE 20/80 blend was far smaller than that of the dispersed PE phase for PVDF/PE 80/20 blend.

The PVDF/PE 20/80 blend showed a monotonous particle size distribution of the dispersed PVDF domains and washer-like halos around etched dispersed phase which is indicative of elongated interfaces during sample fracturing and relatively strong interface. This observation may be attributed to solidification process. According to literature, crystallization temperatures of the PVDF and LLDPE are about 125–150 °C [30–32] and 100–110 °C [33, 34], respectively. Therefore when the 20/80 blend is cooled after melt mixing, the PVDF domains are crystallized before than PE matrix, resulting to compressing of the solid PVDF domains during the PE matrix solidification leading to physical interaction at the interface. On the other hand, in PVDF/PE 80/20 blend, crystallization and shrinkage of PE droplets after solidification of PVDF matrix leads to lower interaction at the interface.

As it was observed un-compatibilized blends represent relatively broad particle size distribution of the dispersed phases and the sharp interface regions between the phases are indicative of high interfacial tension between the components. For matrix-dispersed compositions, there is also evidence of poor interfacial bonding leading to some of droplets being detached from the surrounding matrix, leaving holes on the fractured surface under the fast cryogenic fracture or lying loose on the surface. It seems that the presence of PEMA improved the interaction between phases more or less in different compositions. As evidence, the particle size of the PE droplets of 80/20 blend decreased from about 7 μm (Fig. 7a) to about 5.5 μm (Fig. 7a') after compatibilization and also they exhibited

Fig. 7 SEM micrographs of un-compatible and compatible PVDF/PE blends: **a** 80/20, **a'** 80/15/5, **b** 70/30, **b'** 70/25/5, **c** 60/40, **c'** 60/35/5, **d** 50/50, **d'** 50/45/5, **e** 40/60, **e'** 40/55/5, **f** 20/80, **f'** 20/75/5

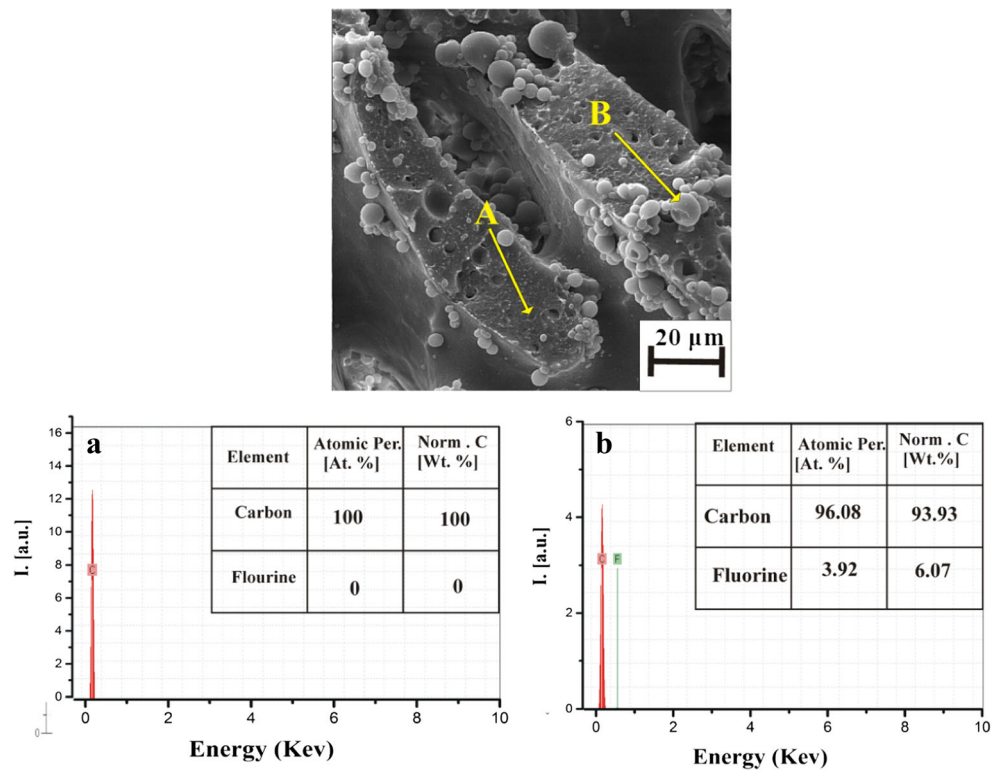


narrower particle size distribution. The results show that the big dispersed spherical particles of PE changed to elongated semi-continuous domains after addition of PEMA to 70/30 blend, confirming the results of continuity index analysis. Compatibilization did not clearly change the co-continuous morphology of 60/40 blend, as it was predicted using rheological analysis. The co-continuous morphology of 50/50 blend altered to dispersion of PVDF particles in PE matrix after compatibilization. This alteration was understood to be responsible for decreased elasticity and increased damping factor (Figs. 4 and 5). For 40/60 blend (a PE-rich blend) compatibilization also decreased the size of PVDF dispersed domains. For 20/80 (another PE-rich blend) compatibilization had less effect on the morphology. Considering the rheological behavior and morphological alteration in all the

compositions, it can be seen that compatibilization had higher effect on PE-rich blends than those of PVDF-rich blends. It may be due to the easier diffusion of PEMA towards the interface through PE matrix compared to PVDF matrix.

Figure 7 (c and c') indicates that for un-compatible and less for compatible 60/40 blend there are some spherical particles left on the etched surface. Since SEM images have been taken after etching of the PVDF phase, these spherical particles cannot be the PVDF particles and they should be trapped PE particles in continuous PVDF phase inside the continuous PE phase. In other words, the real morphology of these samples is phase within a phase within a phase, in which both PVDF and PE phases are continuous and some part of PE phase is dispersed within the PVDF phase. SEM-EDX analysis was employed to further analyze the nature of

Fig. 8 SEM-EDX spectra of the 60/40 blend: **a** the spectrum corresponds to the A region (PE matrix) and **b** the spectrum corresponds to the B region (individual dispersed particles)



these dispersed particles. Fig. 8 shows the EDX spectra together with the atomic percentage of Carbon (C) and Fluorine (F) inside, corresponding to two different parts in the 60/40 blend sample (A: continuous PE phase and B: spherical particles left on the surface). A single peak, corresponding to Carbon (C), can be seen in Fig. 8a, showing the characteristics of pure PE surface. A negligible trace of Fluorine (F; 3.92 atm.%) together with the Carbon (C; 96.08 atm.%) can be seen in the surface of the individual particles (Fig. 8b). This shows that, the individual particles are PE particles and the trace of Fluorine is related to the PVDF chains at the surface of PE particles. It was understood that the difference in melting temperatures of PVDF and PE phases is the main reason behind of development of this type of morphology. During the melt blending process, after simultaneous feeding of PVDF and PE phases, PE phase with lower melting temperature (120–125 °C [30–32]) melts at first and forms the continuous phase with the solid particles of PVDF within PE

phase. After melting of the PVDF phase at about 170 °C [34] it dominates the PE phase to form continuous phase inside the PE phase based on the composition. In this stage some domains of PE phase are trapped in PVDF phase and they don't reach to each other and/or to continuous PE phase. These are schematically illustrated in Fig. 9.

To investigate the effect of feeding sequence on the morphology of 50/50 blend two other 50/50 blends were also prepared using the second and third types of feeding orders (Table 1). For PVDF/(PE) 50/50 and (PVDF)/PE 50/50 samples the PE and PVDF phases were fed at first, respectively and then the other phase was fed after melting of the first phase. Interestingly the SEM images showed that both the blends exhibited a clear matrix-dispersed morphology in which the PVDF phase is dispersed in PE matrix, without trapped PE particles in PVDF phase (Fig. 10). Therefore the equilibrium morphology in this composition is matrix-dispersed morphology without trapped PE particles within

Fig. 9 Schematic representation of the formation of PE particles within continuous PVDF phase

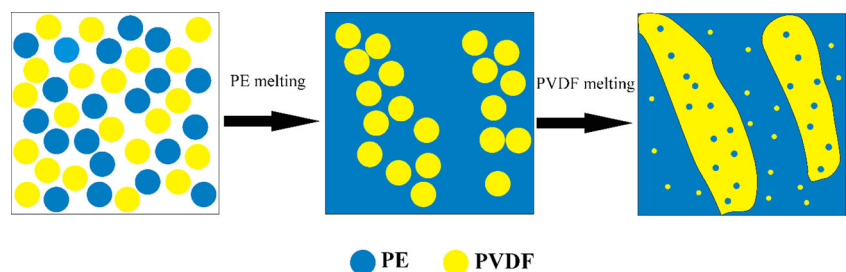
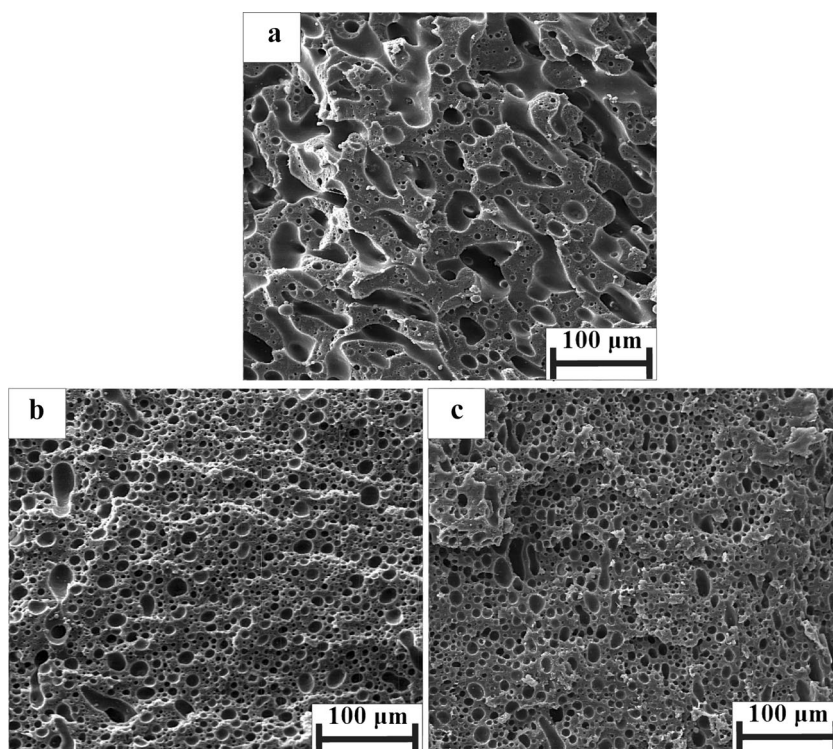


Fig. 10 SEM images of PVDF/PE 50/50 blends prepared using three different feeding orders. **a** Feeding order 1 (simultaneously feeding), **b** Feeding order 2 (PE before) and **c** Feeding order 3 (PVDF before)



the PVDF phase. From these results it can also be concluded that in the case of simultaneously feeding of PVDF and PE phases, trapping of PE particles within the PVDF phase increases and decreases the apparent volume fractions of PVDF and PE phases, respectively, leading to creation of semi co-continuous morphology.

Conclusion

Relationship between the microstructure and linear viscoelastic properties of PVDF/PE blends in a wide range of composition were studied in detail. The effect of PEMA compatibilizer on rheology and morphology of these blends was also studied. The obtained results were conducted to the following conclusions:

Using rheological analysis, it was predicted that the matrix-dispersed morphology of PVDF/PE blends, at low PE contents, would alter to co-continuous morphology at intermediate compositions and again change to dispersed-matrix morphology with further increase in PE content. The results of SEM experiments as well as continuity index analysis, conducted via selective extraction method, confirmed the results of rheological studies.

Compatibilization induced morphology alteration, particularly near the phase inversion region, was also well predicted using rheological analysis and supported via direct morphological observations, so that compatibilization narrowed the co-continuity region. Considering alteration in rheology and

morphology of all the compositions indicated that compatibilization had higher effect on PE-rich blends than those of PVDF-rich blends.

It was shown that the feeding sequence had a distinct effect on the morphology of the blends near the phase inversion region. Feeding of PVDF and PE phases one after another led to dispersion of PVDF particles in continuous PE phase, while, one step feeding of PVDF and PE led to a complicated morphology in which both the PVDF and PE phases were continuous and the continuous PVDF phase consisted of some PE dispersed particles. Different melting and crystallization temperature range of PVDF and PE phases was understood to be the main reason of this observation.

References

1. Willemsse RC, Ramaker EJJ, Dam JV, Posthuma de Boer A (1999) Morphology development in immiscible polymer blends: initial blend morphology and phase dimensions. *Polymer* 40:6651–6659
2. Utracki LA (1990) *Polymer alloys and blends: thermodynamics and rheology*. Hanser, Munich
3. Sperling LH (1997) *Polymeric multicomponent materials*. Wiley, New York
4. Han CD (1981) *Multiphase flow in polymer processing*. Academic Press, New York
5. Razavi Aghjeh MK, Khodabandelou M, Khezrefaridi M (2009) Rheology and morphology of high impact polystyrene/polyethylene blends and the effect of compatibilization on their properties. *J Appl Polym Sci* 114:2235–2245

6. Joseph S, Thomas S (2003) Morphology development and mechanical properties of polystyrene/polybutadiene blends. *Eur Polym J* 39:115–125
7. Fina A, Han Z, Saracco G, Gross U, Mainil M (2012) Morphology and conduction properties of graphite-filled immiscible PVDF/PP-g-MA blends. *Polym Adv Technol* 23:1572–1579
8. Cao JP, Zhao J, Zhao X, You F, Yu H, Hu GH, Dang ZM (2013) High thermal conductivity and high electrical resistivity of poly(vinylidene fluoride)/polystyrene blends by controlling the localization of hybrid fillers. *Compos Sci Technol* 89:142–148
9. Huang J, Mao C, Zhu Y, Jiang W, Yang X (2014) Control of carbon nanotubes at the interface of a co-continuous immiscible polymer blend to fabricate conductive composites with ultralow percolation thresholds. *Carbon* 73:267–274
10. Li Y, Shimizu H (2008) Conductive PVDF/PA6/CNTs nanocomposites fabricated by dual formation of co-continuous and nanodispersion structures. *Macromolecules* 41:5339–5344
11. Zhao X, Zhao J, Cao JP, Wang X, Chen M, Dang ZM (2013) Tuning the dielectric properties of polystyrene/poly(vinylidene fluoride) blends by selectively localizing carbon black nanoparticles. *J Phys Chem* 117:2505–2515
12. Yang J, Feng C, Dai J, Zhang N, Huang T, Wang Y (2012) Compatibilization of immiscible nylon 6/poly(vinylidene fluoride) blends using graphene oxides. *Polym Int* 62:1085–1093
13. Sumita M, Sakata K, Asai S, Miyasaka K, Nakagawa H (1991) Dispersion of fillers and the electrical conductivity of polymer blends filled with carbon black. *Polym Bull* 25:265–271
14. Su C, Xu L, Zhang C, Zhu J (2011) Selective location and conductive network formation of multiwalled carbon nanotubes in polycarbonate/poly(vinylidene fluoride) blends. *Compos Sci Technol* 71:1016–1021
15. Zhang C, Yi XS, Yui H, Asai S, Sumita M (1998) Selective location and double percolation of short carbon fiber filled polymer blends: high-density polyethylene/isotactic polypropylene. *Mater Lett* 36:186–190
16. Wang D, Bao Y, Zha JW, Zhao J, Dang ZM, Hu GH (2012) Improved dielectric properties of nanocomposites based on poly(vinylidene fluoride) and poly(vinyl alcohol)-functionalized graphene. *ACS Appl Mater Interfaces* 4:6273–6279
17. Mohamadi S, Sharifi Sanjani N, Foyouhi A (2013) Evaluation of graphene nanosheets influence on the physical properties of PVDF/PMMA blend. *J Polym Res* 20:46–56
18. He F, Lau S, Chan HL, Fan J (2009) High dielectric permittivity and low percolation threshold in nanocomposites based on poly(vinylidene fluoride) and exfoliated graphite nanoplates. *Adv Mater* 21:710–715
19. Lin X, Fan LL, Zhao J, Dang ZM, Ren DY (2015) Effect of the compatibility on dielectric performance and breakdown strength of poly(vinylidene fluoride)/low-density polyethylene blends. *J Appl Polym Sci* 132:42507
20. Kaseem M, Hamad K, Yang HW, Lee YH, Deri F, Ko YG (2015) Melt rheology of poly(vinylidene fluoride) (PVDF)/low density polyethylene (LDPE) blends. *Polym Sci Ser A* 57:233–238
21. Omonov TS, Harrats C, Moldenaers P, Groeninckx G (2007) Phase continuity detection and phase inversion phenomena in immiscible polypropylene/polystyrene blends with different viscosity ratios. *Polymer* 48:5917
22. Faker M, Razavi Aghjeh MK, Ghaffari M, Seyyedi SA (2008) Rheology, morphology and mechanical properties of polyethylene/ethylene vinyl acetate copolymer (PE/EVA) blends. *Eur Polym J* 44:1834–1842
23. Sarazin P, Favis BD (2003) Morphology control in co-continuous poly(L-lactide)/ polystyrene blends: a route towards highly structured and interconnected porosity in poly(L-lactide) materials. *Biomacromolecules* 4:1669–1679
24. Mehrabi Mazidi M, Razavi Aghjeh MK (2015) Effects of blend composition and compatibilization on the melt rheology and phase morphology of binary and ternary PP/PA6/EPDM blends. *Polym Bull* 72:1975–2000
25. Basseri G, Mehrabi Mazidi M, Hosseini F, Razavi Aghjeh MK (2014) Relationship among microstructure, linear viscoelastic behavior and mechanical properties of SBS triblockcopolymer compatibilized PP/SAN blend. *Polym Bull* 71:465–486
26. Krache R, Benachour D, Potschke P (2004) Binary and ternary blends of polyethylene, polypropylene and polyamide 6.6: the effect of compatibilization on the morphology and rheology. *J Appl Polym Sci* 94:1976–1985
27. Hemmati M, Nazokdast H, Shariatpanahi H (2001) Study on morphology of ternary polymer blends. II Effect of composition. *J Appl Polym Sci* 82:1138–1146
28. Wu D, Zhang Y, Zhang M, Zhou W (2008) Phase behavior and its viscoelastic response of polylactide/poly (ε-caprolactone) blend. *Eur Polym J* 44:2171–2183
29. Li R, Yu W, Zhou C (2006) Rheological characterization of droplet-matrix versus co-continuous morphology. *J Macromol Sci Phys* 45:889–898
30. Achaby MEL, Arrakhiz FZ, Vaudreuil S, Essassi EM, Qaiss A, Bousmina M (2013) Preparation and characterization of melt-blended graphene nanosheets–poly(vinylidene fluoride) nanocomposites with enhanced properties. *J Appl Polym Sci* 127:4697–4707
31. Ke K, Wang Y, Yang W, Xie BH, Yang MB (2012) Crystallization and reinforcement of poly(vinylidene fluoride) nanocomposites: role of high molecular weight resin and carbon nanotubes. *Polym Test* 31:117–126
32. Li J, Wu X, Liu Z (2013) Non-isothermal crystallization of poly(vinylidene fluoride)/multiwalled carbon nanotube composites. *Int J Polym Anal Charact* 18:83–92
33. Furukawa T, Sato H, Kita Y, Matsukawa K, Yamaguchi H, Ochiai S, Siesler HW, Ozaki Y (2006) Molecular structure, crystallinity and morphology of polyethylene/polypropylene blends studied by Raman mapping, scanning electron microscopy, wide angle x-ray diffraction and differential scanning calorimetry. *Polym J* 38:1127–1136
34. Krupa I, Luyt AS (2000) Thermal properties of uncross-linked and cross-linked LLDPE/wax blends. *Polym Degrad Stab* 70:111–117